Time-integrated Polarizations of Gamma-ray Burst Prompt Phase

Ruo-Yu Guan

Department of Astronomy, School of Physics, Huazhong University of Science and Technology

Abstract

During the prompt phase, the polarization properties of gamma-ray bursts (GRBs) offer key insights into their emission mechanisms and magnetic field configurations. Accounting for the time evolution of the Stokes parameters can modify the inferred time-integrated polarization degree (PD) relative to estimates constructed from time-integrated spectra. For POLAR-2, the model predicts time-integrated PDs of approximately 40–50% for the High-energy Polarimetry Detector (HPD) and 30–40% for the Low-energy Polarimetry Detector (LPD), assuming large-scale ordered magnetic fields. Modeling with ordered magnetic fields (toroidal or aligned) highlights the importance of time-evolving polarization.

A multi-window fitting approach analyzing light curves, PD, and polarization angle (PA) for 23 GRBs demonstrates that synchrotron radiation in ordered fields explains most observed PDs, averaging ∼44% for aligned fields and ∼49% for toroidal fields. GRBs with strong ($\sim 90°$) PA rotations favor aligned magnetic fields, while those without strong rotations show comparable predictions for both configurations. Within this sample, models based on synchrotron radiation in ordered magnetic fields are consistent with most of the available polarization observations under the reported observational constraints.

Background

Gamma-ray bursts (GRBs) are powerful cosmic explosions whose prompt emissions provide insights into emission mechanisms and magnetic fields. Polarization studies reveal a wide range of polarization degrees (PDs), typically from ∼10% (e.g., POLAR observations) to ∼40% (e.g., AstroSat observations), depending on the instrument and spectral properties. The synchrotron emission model with ordered magnetic fields explains most observations but struggles with outliers like GRB 110721A and GRB 180427A (Guan & Lan, 2023). Time-resolved and multi-window analyses are essential to address these challenges.

Physical Picture

The emission model, proposed by Uhm & Zhang (2015, 2016); Uhm et al. (2018), consists of a thin, radially expanding relativistic jet shell emitting photons continuously from $R_{\rm on}$ to $R_{\rm off}$.

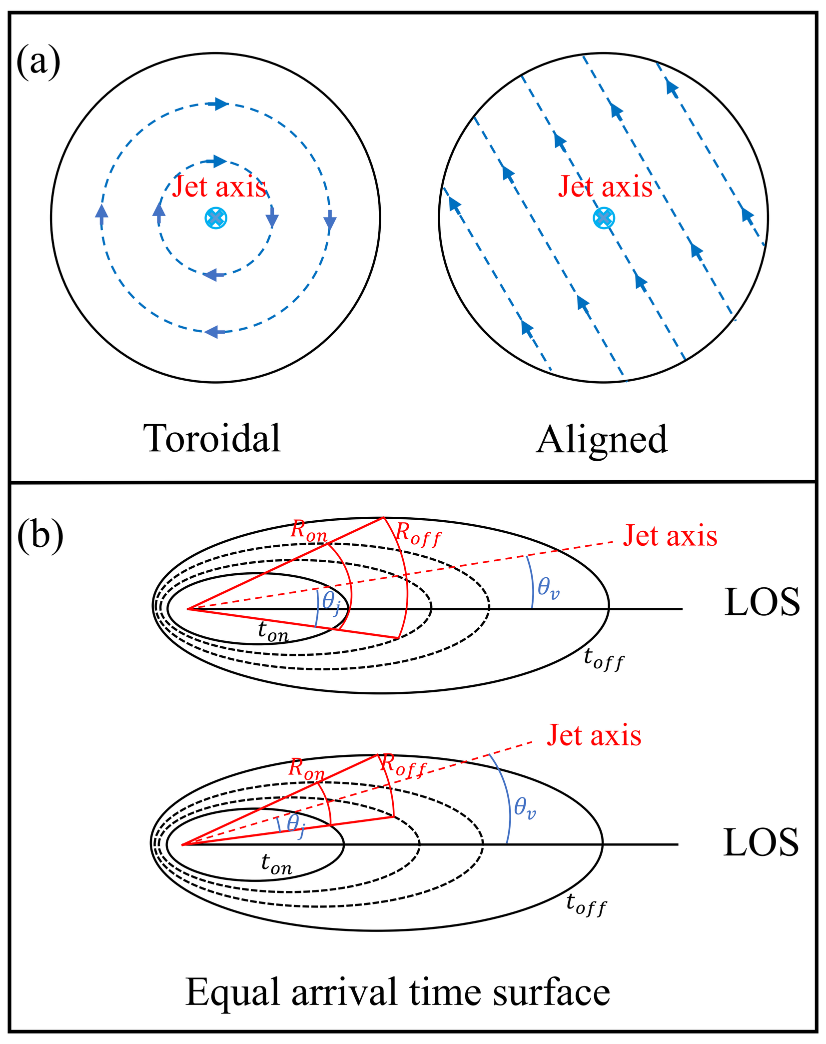

Figure 1. Taken from Sui & Lan (2024). (a) Schematic of two types of ordered magnetic fields on the jet surface, with blue arrows showing field directions and the cross marking the jet axis. (b) Cross-sections of Equal Arrival Time Surfaces (EATSs) for on-axis (top) and off-axis (bottom) observations, with radiation spanning from $t_{\rm on}$ to $t_{\rm off}$.

As the jet shell expands, adiabatic expansion and magnetic reconnection reduce the magnetic field strength, while the bulk Lorentz factor is parametrized as a power law of radius (Spruit et al., 2001; Drenkhahn, 2002).

$$B'(r) = B'_0 \left(\frac{r}{r_0}\right)^{-b} \tag{1}$$

$$\Gamma(r) = \Gamma_0 \left(\frac{r}{r_0}\right)^{s} \tag{2}$$

The model assumes single-energy electrons with Lorentz factor $\gamma_{\rm ch}$ in the comoving frame. Two prescriptions for the radial evolution of $\gamma_{\rm ch}$ are adopted to describe the commonly observed hard-to-soft ("i" model) and intensity-tracking ("m" model) patterns of E_p evolution (Uhm et al., 2018). For the "i" model, $\gamma_{\rm ch}$ follows a single power law:

$$\gamma_{\rm ch}(r) = \gamma^0_{\rm ch}\left(\frac{r}{r_0}\right)^{g} \tag{3}$$

For the "m" model, $\gamma_{\rm ch}$ follows a broken power law:

$$\gamma_{\rm ch}(r) = \gamma^m_{\rm ch}\begin{cases}(r/r_m)^{g}, & r \le r_m,\\ (r/r_m)^{-g}, & r \ge r_m\end{cases} \tag{4}$$

Model Description

The polarization model follows Lan & Dai (2020) and Sui & Lan (2024). The time- and energy-resolved Stokes parameters are given by:

$$F_\nu = \frac{1+z}{4\pi D_L^2}\int \mathcal{D}^3 \sin\theta d\theta \int \frac{N P'_0 H_{en}(x)\sin\theta'_B}{4\pi} d\phi, \tag{5}$$

$$Q_\nu = \frac{1+z}{4\pi D_L^2}\int \mathcal{D}^3 \sin\theta d\theta \int \Pi_{p,b}\cos 2\chi_p \frac{N P'_0 H_{en}(x)\sin\theta'_B}{4\pi} d\phi, \tag{6}$$

$$U_\nu = \frac{1+z}{4\pi D_L^2}\int \mathcal{D}^3 \sin\theta d\theta \int \Pi_{p,b}\sin 2\chi_p \frac{N P'_0 H_{en}(x)\sin\theta'_B}{4\pi} d\phi. \tag{7}$$

To obtain the time- and energy-integrated polarization degree Π (PD) and polarization angle χ (PA), we do the following integration:

$$\bar{O} = \frac{\int_{T_5}^{T_{95}}\int_{\nu_1}^{\nu_2} O_\nu d\nu dt_{\rm obs}}{\int_{T_5}^{T_{95}} dt_{\rm obs}}, \text{ where } O \text{ can be } F, Q, \text{ or } U. \tag{8}$$

Thus,

$$\Pi = \frac{\sqrt{(\bar{Q}^2+\bar{U}^2)}}{\bar{F}}, \tag{9}$$

$$\chi = \frac{1}{2}\arctan\left(\frac{\bar{U}}{\bar{Q}}\right). \tag{10}$$

Results

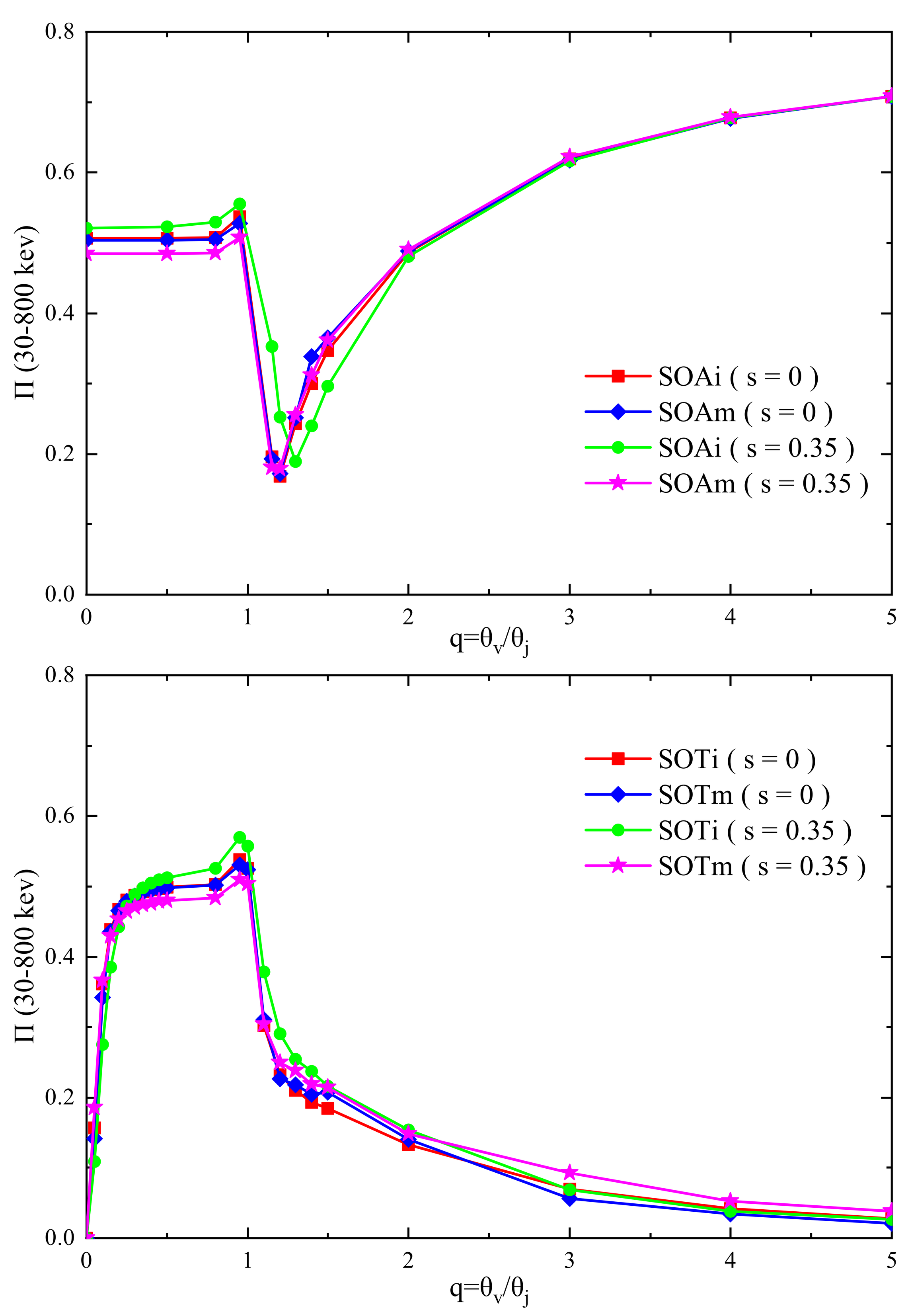

Figure 2. Taken from Sui & Lan (2024). Time-integrated PD (Π) versus $q \equiv \theta_V/\theta_j$ for the POLAR-2 HPD (30–800 keV), for aligned (top) and toroidal (bottom) ordered magnetic fields. "SO" denotes synchrotron emission in an ordered field; A/T and i/m denote the field configuration and E_p-evolution prescription, respectively.

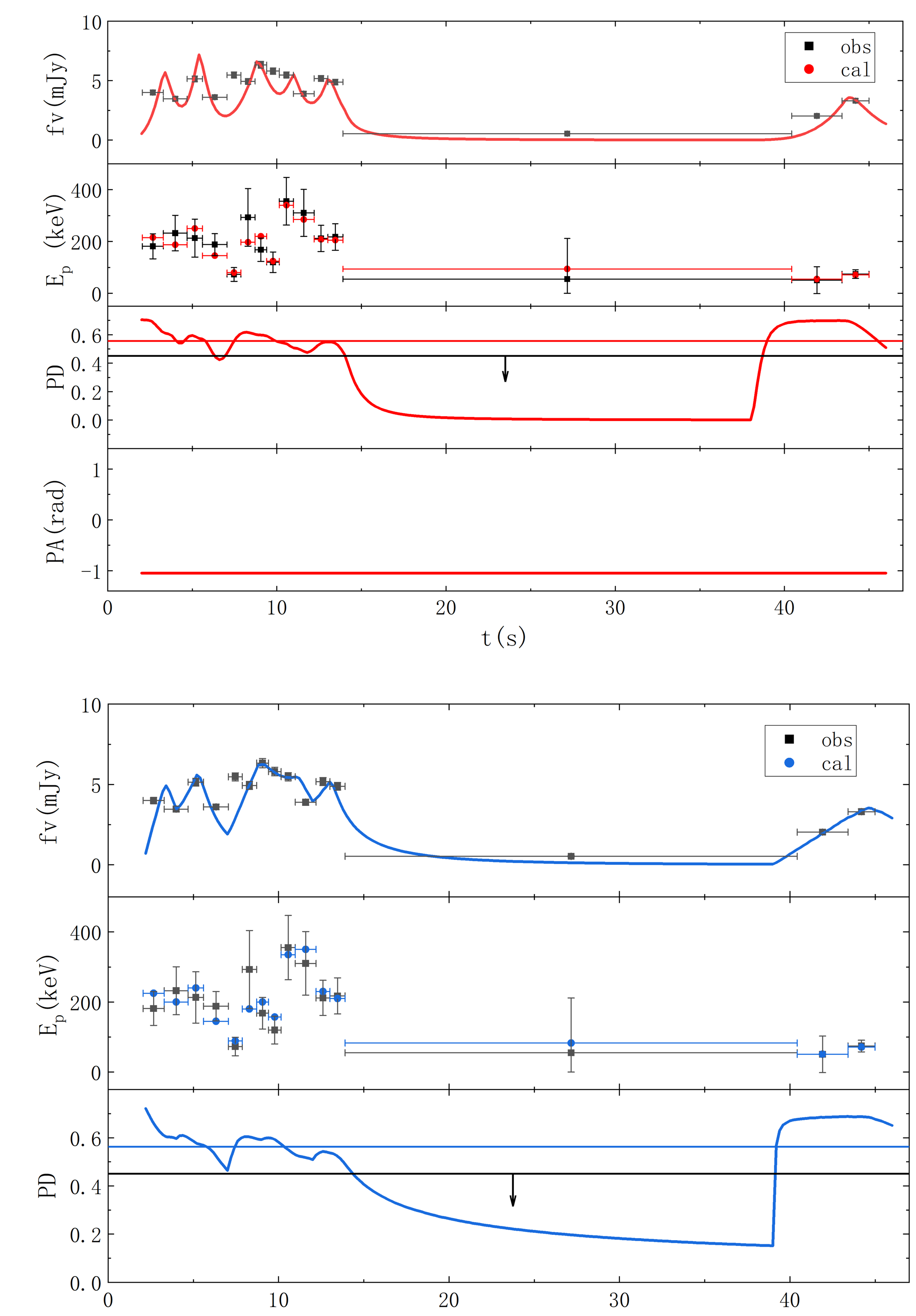

Figure 3. Taken from Wang et al. (2024). Multi-window fitting results for GRB 160325A. The upper panels show the aligned-field case (light curve, E_p, PD, and PA), and the lower panels the toroidal-field case (light curve, E_p, and PD). Symbols show observations and colored curves show the corresponding model fits; horizontal lines indicate the observed and predicted time-integrated PDs.

Summary

- For the 23-GRB multi-window sample, the predicted mean time-integrated PDs are approximately 44% for aligned magnetic fields and 49% for toroidal magnetic fields, with predictions for 22 of the 23 bursts consistent with the corresponding observational constraints.
- For GRB 170206A, the comparatively low observed time-resolved and time-integrated PDs suggest that a random magnetic-field component may coexist with the ordered component.
- Within this sample, synchrotron radiation models with ordered magnetic fields can reproduce most of the available polarization observations, providing constraints on the radiation mechanism and magnetic-field configuration.
- Time-resolved multi-window fitting provides more physically informed PD predictions by simultaneously incorporating light curves, spectral evolution, and polarization evolution.
- If the reported strong ($\sim 90°$) PA rotations are reliable, they favor a large-scale ordered aligned-field component, which, within this magnetic-reconnection framework, may in turn favor a magnetar central-engine scenario.

References

Drenkhahn, G. 2002, A&A, 387, 714

Guan, R. Y., & Lan, M. X. 2023, A&A, 670, A160

Lan, M.-X., & Dai, Z.-G. 2020, ApJ, 892, 141

Spruit, H. C., Daigne, F., & Drenkhahn, G. 2001, A&A, 369, 694

Sui, L.-Q., & Lan, M.-X. 2024, MNRAS, 529, 4287

Uhm, Z. L., & Zhang, B. 2015, ApJ, 808, 33

—. 2016, ApJ, 825, 97

Uhm, Z. L., Zhang, B., & Racusin, J. 2018, ApJ, 869, 100

Wang, X., Lan, M.-X., Tang, Q.-W., Wu, X.-F., & Dai, Z.-G. 2024, arXiv e-prints, arXiv:2411.09106